Fungal Genetics and Biology 81 (2015) 73–81

Contents lists available at ScienceDirect

Fungal Genetics and Biology

journal homepage: www.elsevier.com/locate/yfgbi

Regular Articles

Development of an *Agrobacterium*-mediated transformation system for the cold-adapted fungi *Pseudogymnoascus destructans* and *P. pannorum*

Tao Zhang [a], Ping Ren [a], Vishnu Chaturvedi [a,b], Sudha Chaturvedi [a,b,*]

[a] Mycology Laboratory, Wadsworth Center, New York State Department of Health, Albany, NY, USA
[b] Department of Biomedical Sciences, School of Public Health, University at Albany, Albany, NY, USA

ARTICLE INFO

Article history:
Received 2 October 2014
Revised 21 May 2015
Accepted 23 May 2015
Available online 5 June 2015

Keywords:
Agrobacterium tumefaciens-mediated transformation (ATMT)
White-nose syndrome (WNS)
Homologous recombination
Urease

ABSTRACT

The mechanisms of cold adaptation by fungi remain unknown. This topic is of high interest due to the emergence of white-nose syndrome (WNS), a skin infection of hibernating bats caused by *Pseudogymnoascus destructans* (*Pd*). Recent studies indicated that apart from *Pd*, there is an abundance of other *Pseudogymnoascus* species in the hibernacula soil. We developed an *Agrobacterium tumefaciens*-mediated transformation (ATMT) system for *Pd* and a related fungus *Pseudogymnoascus pannorum* (*Pp*) to advance experimental studies. *URE1* gene encoding the enzyme urease was used as an easy to screen marker to facilitate molecular genetic analyses. A Uracil-Specific Excision Reagent (USER) Friendly pRF-HU2 vector containing *Pd* or *Pp ure1*::hygromycin (*HYG*) disruption cassette was introduced into *A. tumefaciens* AGL-1 cells by electroporation and the resulting strains were co-cultivated with conidia of *Pd* or *Pp* for various durations and temperatures to optimize the ATMT system. Overall, 680 *Pd* (0.006%) and 1800 *Pp* (0.018%) transformants were obtained from plating of 10^7 conidia; their recoveries were strongly correlated with the length of the incubation period (96 h for *Pd*; 72 h for *Pp*) and with temperature (15–18 °C for *Pd*; 25 °C for *Pp*). The homologous recombination in transformants was 3.1% for *Pd* and 16.7% for *Pp*. The availability of a standardized ATMT system would allow future molecular genetic analyses of *Pd* and related cold-adapted fungi.

1. Introduction

Pseudogymnoascus destructans (*Pd*) is the etiologic agent of white-nose syndrome (WNS), a skin infection of hibernating bats. This pathogen has caused unprecedented reductions in the abundance of the bat populations in the northeastern United States since 2006, with up to 95% mortality in some hibernacula (Blehert et al., 2009; Chaturvedi et al., 2010; Frick et al., 2010; Blehert, 2012). *Pd* is a newly recognized fungus that is well adapted to growing under cold conditions found in caves and mines. It secrets proteolytic enzymes documented in other pathogenic fungi to cause vertebrate skin infections. The pathogen appears to have a clonal population in the US (Rajkumar et al., 2011; Ren et al., 2012). However, the precise mechanisms by which *Pd* survives and invades the skin of the hibernating bats are not clear. Phylogenetic analyses of hibernacula soil revealed large number of *Pseudogymnoascus* spp., which have not been implicated in WNS (Minnis and Lindner, 2013). These results indicated that *Pd* possess certain unique virulence repertoire to cause disease in bats, which seems to be missing in other *Pseudogymnoascus* spp. It is also conceivable that mammalian or non-mammalian hosts are yet to be identified for other *Pseudogymnoascus* spp.

Recently, integrated genome profile analyses of *Pd* and *Geomyces pannorum* (re-named as *Pseudogymnoascus pannorum;* accession no. AYKR00000000) yielded preliminary information on the fundamental biological capabilities including pathogenicity, cold adaptation, and regulation mechanisms (Chibucos et al., 2013). However, follow-up experimental studies are not yet possible due to unavailability of an efficient transformation system. The lack of molecular tools also extends to other fungi inhabiting the cold environment.

The *Agrobacterium tumefaciens*-mediated transformation system (ATMT) has been successfully used for molecular genetic studies of yeasts and filamentous fungi, including *Saccharomyces* (Piers et al., 1996), *Cryptococcus* (McClelland et al., 2005), *Coccidioides* (Abuodeh et al., 2000), *Aspergillus* (Gouka et al., 1999; Michielse et al., 2005), *Trichophyton* (Yamada et al., 2009), *Fusarium* (Mullins et al., 2001), *Glomus* (Helber and Requena, 2008), *Oculimacula* (Eckert et al., 2005) and *Verticillium* (Dobinson et al., 2004). ATMT also has been shown to be an important alternative to other fungal transformation systems, as it yields a high number of transformants, is easier to perform, does not require special

* Corresponding author at: Mycology Laboratory, Wadsworth Center, New York State Department of Health, Albany, NY, USA.
E-mail address: sudha.chaturvedi@health.ny.gov (S. Chaturvedi).

http://dx.doi.org/10.1016/j.fgb.2015.05.009
1087-1845/

equipment, and is characterized by a high frequency of homologous recombination (Frandsen, 2011).

The enzyme urease encoded by *URE1* gene is an important virulence factor for the fungal pathogens *Cryptococcus neoformans* and *Coccidioides posadasii* (Olszewski et al., 2004; Mirbod-Donovan et al., 2006) and the bacterial pathogens *Helicobacter pylori* and *Proteus mirabilis* (Jones et al., 1990; Eaton et al., 1991; Tsuda et al., 1994). It has been reported that *Pd* also secretes significant amounts of urease, but its precise function in either the saprophytic or parasitic life of this fungus is not clear (Chaturvedi et al., 2010; Reynolds and Barton, 2014). In this report, we have used the urease-encoding gene *URE1* as an easily screenable marker to develop an ATMT system for cold-adapted fungi, which would prove valuable for future molecular genetics and pathogenic studies of *Pd* and other related species in this genus.

2. Materials and methods

2.1. Strains, plasmids and media

All strains and plasmids used in this study are listed in Table 1. *P. destructans* (*Pd*) and *P. pannorum* (*Pp*) strains were routinely maintained on yeast extract peptone dextrose (YPD) agar and stored in 15% glycerol at −70 °C. Potato dextrose agar (PDA; Difco), Christensen's urea agar (Sigma–Aldrich), YNB medium [2% glucose, 0.17% yeast nitrogen base without amino acids and ammonium sulfate (Cat. no. 233520) and 2% agar], YNB-U (0.227% urea as sole source of nitrogen) were used to assess phenotypes of mutants and wild type (WT) strains of *Pd* and *Pp*. The induction medium (IM) used for co-cultivation experiments was composed of $K_2HPO_4{\cdot}3H_2O$ 1.9 g, K_2HPO_4 2.05 g, $MgSO_4{\cdot}7H_2O$ 0.5 g, $(NH_4)_2SO_4$ 0.5 g, glucose 1.8 g, 4% (w/v) glycerol and a final concentration of 40 mM MES hydrate (Sigma–Aldrich) per liter (Zhang et al., 2013). Yeast extract broth (YEB) used for culture of *A. tumefaciens* (AGL-1) cells contained 10 g peptone, 1 g yeast extract, 5 g sucrose and 0.5 g $MgSO_4{\cdot}7H_2O$ per liter and adjusted to pH 7.0.

2.2. URE1 gene characterization from Pd and Pp

DNA sequences of *PdURE1* and *PpURE1* were first obtained from *Pd* (http://broadinstitute.org/annotation/genome/Geomyces_destructans/MultiHome.html) and *Pp* (http://fungalgenomics.concordia.ca/fungi/Gpan.php) genome databases and then blasted

Table 1
Strains, plasmids and oligonucleotides used in this study.

Strains	Description	Source
E. coli Top10	lacx74 recA1 deoR F – mcrA Δ (mrr-hsdRMS-mcrBC) ϕ80 lacZΔM15Δ araD139Δ (ara-leu)7697 galU galK	Invitrogen
Agrobacetrium tumefaciens (AGL-1)	Genotype-AGL0 recA::bla pTiBo542deltaT Mop+ CbR	Dr. Seogchan Kang, University Park, PA, USA
Pseudogymnoascus destructans (*Pd*) M1379	Wild type strain	Bat skin (Chibucos et al., 2013)
Pseudogymnoascus pannorum (*Pp*) M1372	Wild type strain	Soil (UAMH1062) (Chibucos et al., 2013)
Pdure1–10	ure1 mutant of *Pd*	This study
Pdure1–25	ure1 mutant of *Pd*	This study
Ppure1–4	ure1 mutant of *Pp*	This study
Ppure1–11	ure1 mutant of *Pp*	This study
Plasmid	Description	Source
pRF-HU2	Vector for targeted gene replacement containing *HYG* gene as selection marker	(Frandsen et al., 2008)
pPdure1::HYG	5′ and 3′ prime arms of *PdURE1* gene cloned into pRF-HU2	This study
pPpure1::HYG	5′ and 3′ prime arms of *PpURE1* gene cloned into pRF-HU2	This study
Oligonucleotides	Sequence (5′–3′)	Purpose
V2149a	GGTCTTAAUTTTAGGCGGAGCTATGAC	*pPdure1::HYG* vector construction
V2150a	GGCATTAAUAAGGGCGTTGATGATGAC	*pPdure1::HYG vector construction*
V2151a	GGACTTAAUTATGTTGCAGGCTTTGGA	*pPdure1::HYG* vector construction
V2152a	GGGTTTAAUGATCTGGCATCATATCGTC	*pPdure1::HYG* vector construction
V2171	AGCTGCGCCGATGGTTTCTACAA	Hyg^+ transformant screening and *HYG* probe for Southern analysis of *Ppure1* mutants
V2172	GCGCGTCTGCTGCTCCATACAA	Hyg^+ transformant screening and *HYG* probe for Southern analysis of *Ppure1* mutants
V2173	GGGTTTAAUTGCCACCGCCAATGTATC	*pPpure1::HYG* vector construction
V2174	GGACTTAAUTCATCATCAACGCCCTTA	*pPpure1::HYG* vector construction
V2175	GGCATTAAUACGGTGACGAGGTAGGTT	*pPpure1::HYG* vector construction
V2176	GGTCTTAAUGACGAGGCGGTTGAGGAA	*pPpure1::HYG* vector construction
V2199	CCATACCGTCACGCAGAG	*Ppure1* mutant screening
V2200	AATAAAGGGCGGAAGAGG	*Ppure1* mutant screening
V2201	TAAATCCGTTCTTGATGCCGATATC	*Ppure1* mutant screening
V2202	AATGTTGCGGATCTCATG	*Ppure1* mutant screening
V2203	ATTGTTGATTGGAGTGGTATT	*Pdure1* mutant screening
V2204	CCGCATGTTGTTCTTGCC	*Pdure1* mutant screening
V2205	CATCATCAACGCCCTTAT	*Pdure1* mutant screening
V2206	AGCTCCCATGTCGTGTAA	*Pdure1* mutant screening
V2281	GACCAGTTGCCTAAATGAA	*Pdure1* mutant screening
V2282	GTAAGTATGGGAAGCAGAAA	*Pdure1* mutant screening
V2285	TTTCGGCGTGGGTATGGT	*Ppure1* mutant screening
V2286	TCGGATTCAAGCGACTGG	*Ppure1* mutant screening
V2370	TTCAGTAACGTTAAGTGGATCC	*HYG* probe for Southern analysis of *Pdure1* mutants
V2372	CGCAAGGAATCGGTCAATAC	*HYG* probe for Southern analysis of *Pdure1* mutants

The underlined sequences denote 9-bp long 2-deoxyuridine containing overhangs for directional cloning into pRF-HU2 vector (Frandsen et al., 2008).

against *Pd* M1379 (http://www.ncbi.nlm.nih.gov/nuccore/AYKP00000000) and *Pp* M1372 (http://www.ncbi.nlm.nih.gov/nuccore/AYKR0000 0000) databases to get full-length sequences (Chibucos et al., 2013). Open reading frame (ORF) analysis was carried out using the programs AUGUSTUS (Stanke et al., 2004; Stanke and Morgenstern, 2005) and FGENESH (www.softberry.com). Gene models were manually curated using exon/intron boundary predictions from SPLICEPORT (Dogan et al., 2007). Multiple sequence alignments were created with reference to selected GenBank sequences using the MAFFT program (Katoh et al., 2009). Phylogenetic analysis using the neighbor-joining (NJ) method with 1000 bootstrap replicates was done using MEGA 4.1 (Tamura et al., 2007).

2.3. Vector construction

Genomic DNA from *Pd* and *Pp* cultures was extracted using a modified protocol (Möller et al., 1992). In brief, approximately two loopfuls of the fungal colony was removed from the agar plate and placed in 300 µl of genomic DNA extraction buffer (100 mM Tris [pH 8.0], 10 mM EDTA, 2% SDS, 1.4 M NaCl, 1% CTAB, 0.4 µg/ml proteinase K). The mixture was incubated at 65 °C for 1 h followed by chloroform: isoamyl alcohol (24:1) extraction, and precipitation with isopropanol and washing with 70% ethanol. The precipitated DNA was centrifuged at 12,000 rpm and the resulting pellet was dried under air and dissolved in 50 µl of Tris–EDTA (TE) buffer. The 5′- and 3′-prime arms of the *URE1* gene (approximately 1.5 kb) from *Pd* and *Pp* were PCR amplified using primers that contained 5′-deoxyuridine extensions (Table 1). These PCR amplicons were cloned into the Uracil-Specific Excision Reagent (USER)-Friendly cloning vector pRF-HU2 flanking the hygromycin B resistance (*HYG*) gene under the control of the *Aspergillus nidulans trpC* promoter and terminator. The vector contained the necessary elements (*oriV* and *trfA*) for replication in *Escherichia coli* and *A. tumefaciens* cells (Frandsen et al., 2008; Zhang et al., 2013). The resulting plasmids were designated as *pPdure1::HYG* and *pPpure1::HYG* gene disruption cassettes.

2.4. ATMT transformation procedure

The ATMT transformation of *Pd* and *Pp* was carried out as per published protocols (Gouka et al., 1999; Mullins et al., 2001). In brief, *A. tumefaciens* strain AGL-1 was transformed with *pPdure1::HYG* and *Ppure1::HYG* disruption cassettes by electroporation (Mozo and Hooykaas, 1991). The transformed AGL-1 cells were subsequently grown in YEB broth containing kanamycin (50 µg/ml) for 48 h at 28 °C. One milliliter of the cell culture was spun down and washed with induction medium (IM). Bacterial cells were diluted in IM medium (10 ml) with or without 200 µM acetosyringone (AS; Sigma–Aldrich) to an OD_{600} = 0.30 and incubated (200 RPM) at 28 °C until an OD_{600} = of approximately 0.80 (1×10^8 cells/ml) reached.

Conidia from *Pd* and *Pp* cultures grown in PDA agar for four weeks were harvested by gently scraping fungal growth from the agar surface and passing it through 27G needle to get a suspension of single conidia (Fig. S1A and B). Conidia were counted microscopically and adjusted to concentrations as needed for various experiments. To determine optimum concentration of hygromycin B required for complete inhibition of *Pd* or *Pp* growth, approximately 100 µl of conidial suspension (10^8) were spread on PDA plates containing various concentration of hygromycin B (50–200 µg/ml) and plates were incubated at 15 °C for 1–4 weeks and presence or absence of growth of WT strains of *Pd* or *Pp* was assessed.

For transformation studies, conidia were adjusted to 1×10^7 cells/ml in IM broth with or without AS. Aliquots of 100 µl of *Pd* or *Pp* conidial suspension (1×10^6 conidia) were mixed with an equal volume of AGL-1 cells (1×10^7 cells) carrying either p*Pdure1::HYG* or p*Ppure1::HYG*, and were evenly spread onto sterilized nitrocellulose membranes (Cat. no. D9527, Sigma–Aldrich) placed on IM agar with or without AS. A total of 3 membranes per condition were used. The co-cultivation experiments were performed at various temperatures (10–30 °C) and time intervals (24–96 h). The membranes were then transferred to PDA containing hygromycin (100 µg/ml) as a selection agent for the recovery of putative hygromycin positive (Hyg^+) transformants and cefotaxime (200 µg/ml) to kill the *A. tumefaciens* cells. Representative plates containing putative Hyg^+ *Pd* and *Pp* transformants are shown (Supplementary Fig. S1C and D). The putative Hyg^+ transformants were then streaked on selection medium and plates were incubated at 15 °C for 2 weeks. Representative plates with putative Hyg^+ colonies are shown (Supplementary Fig. S1E and F).

2.5. DNA extraction and analysis

Genomic DNA from the putative Hyg^+ transformants was extracted as described above for the *Pd* and *Pp* WT strains. The transformants were first screened for the presence of the *HYG* gene and then for *ure1::HYG* disruption cassette integration at the homologous site by PCR (Table 1). The PCR conditions were: initial denaturation at 95 °C for 3 min followed by 40 cycles at 94 °C for 30 s, annealing at 55 °C to 63 °C for 30 s (based on primer pair) and extension at 72 °C for 40 s to 3 min (based on amplicon size). The transformants with single *ure1::HYG* integration at the homologous site were further confirmed by Southern analysis. In brief, genomic DNA (~5 µg) was digested with restriction enzymes, fractionated by electrophoresis (1% agarose gel), transferred to a Hybond™-XL nylon membrane (Cat. no. RPN303 S, GE Healthcare), and fixed by UV cross-linking. The membranes were hybridized overnight at 55 °C with *HYG* probe [PCR amplified fragment of *HYG* labeled with ^{32}P-dCTP by random priming (Perkin Elmer)]. Following hybridization, these membranes were washed, dried and visualized using Image Quant Software (Molecular Dynamics Inc.).

2.6. Urease enzyme activity assay

The urease enzyme activities of mutants and WT strains were assessed by inoculating 10 µl of conidial suspensions (10^7 conidia/ml) on Christensen's urea agar tubes and these tubes were incubated at 15 °C for 2 weeks. A color change to bright magenta was indicative of urease production.

For assay of urease enzyme activity, the *ure1* mutant and WT strains were first inoculated in YNB-U broth and incubated at 15 °C for 10 days. Cells were harvested by centrifugation at 10,000 g for 10 min. The cell pellets were washed twice in 50 mM sodium phosphate buffer (pH 7.6) and re-suspended in the same buffer. Cells were disrupted at a setting of 6.5 for 45 s with a FastPrep FP120 apparatus (Bio101 Savant Instruments, Inc., Holbrook, NY). Cellular debris was removed by centrifugation at 12,000g at 4 °C for 15 min, and the supernatant assayed for urease enzyme activity according to the protocol described in the QuantiChrom™ Urease Assay Kit (BioAssay Systems, Hayward, CA, USA). One unit of urease enzyme activity is defined as the amount of enzyme required to hydrolyze one µmol of urea per min at 25 °C. Hydrolysis was measured by monitoring the rate of release of ammonium ions (NH_4^+) plus ammonia (NH_3) from the urea substrate as determined by the Bertholet reaction. All analyses were conducted in triplicates.

Next, we tested if *URE1* gene is involved in urea metabolism. Approximately 10 µl aliquots of serial dilutions of conidial suspension of *Pd* and *Pp* WT and their respective *ure1* mutant strains were spotted on YNB-U medium and plates were incubated at 15 °C for 7 days.

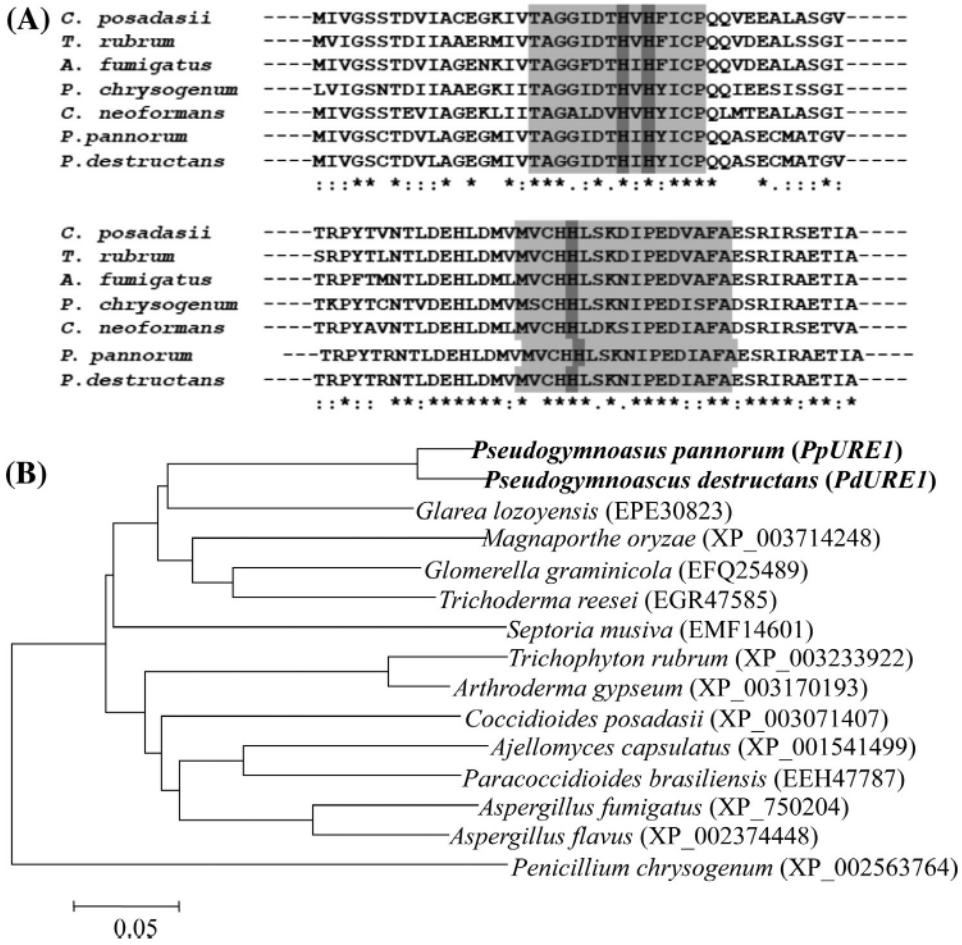

Fig. 1. Multiple alignment and phylogenetic relationship of deduced amino acid sequences of *URE1* of *Pd* and *Pp* with other fungal *URE1* genes. (A) Portions of the amino acid sequences of URE1p were used for multiple alignments, and the sequences corresponding to amino acids 399 to 412 and 513 to 525 are numbered based on *Pp*URE1p. The conserved histidine residues important in binding to the nickel metallocenter (amino acid 406), binding to the substrate (amino acid 408), and catalysis (amino acid 518) are in boldface and marked with a star. (B) The full-length amino acid sequences of URE1p were used to construct a phylogenetic tree by the neighbor-joining method. The bootstrap scores are based on 1000 reiterations. The URE1p from *Penicillium chrysogenum* is used as an outgroup.

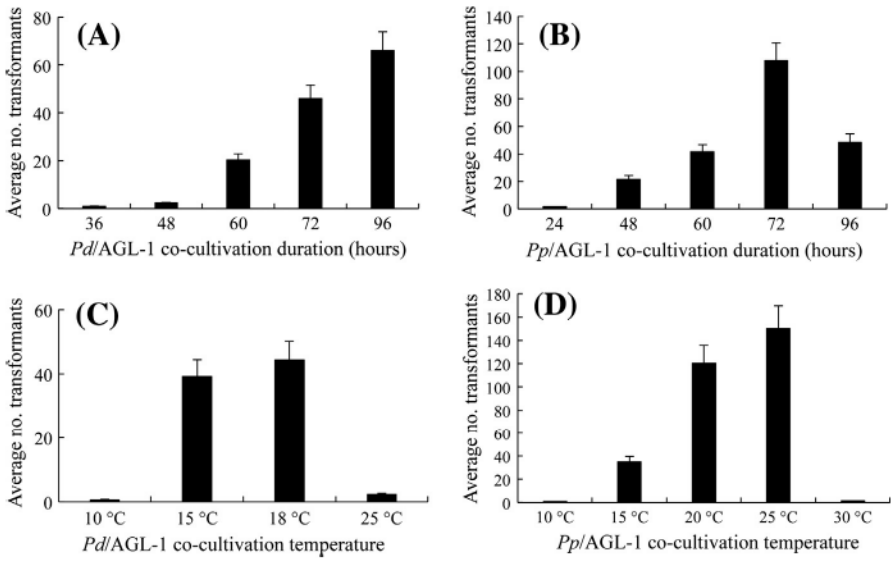

Fig. 2. Co-cultivation parameters for transformation efficiency of *Pd* and *Pp*. (A and B) Effect of co-cultivation duration. *A. tumefaciens* AGL-1 cells grown in IM medium containing AS were mixed with *Pd* or *Pp* conidial suspension at 10:1 ratio and of these suspension, 200 μl was inoculated per plate followed by incubation at 15 °C for *Pd* (A) and at 25 °C for *Pp* (B) for various durations prior to hygromycin selection. Data presented as the average of three plates per treatment. (C and D) Effect of co-cultivation temperatures. *A. tumefaciens* AGL-1 cells grown in IM medium containing AS were mixed with *Pd* or *Pp* conidial suspension at 10:1 ratio and of these 200 μl was inoculated per plate followed by incubation at various temperatures for 72 h prior to hygromycin selection.

2.7. Growth and sporulation studies

The *ure1* mutant and WT strains were assessed for growth at various temperatures. Conidial suspensions were prepared as described above, and adjusted to 10^7 cells/ml. Serial 10-fold dilutions were prepared, and 10 µl of each dilution was spotted onto YPD and PDA agar plates. All agar plates were incubated at 6 °C, 15 °C and 25 °C for 7–14 days. For sporulation, mutant and WT strains were grown on PDA agar at 15 °C for 25 days, scotch tape mounts were prepared and assessed microscopically.

2.8. Statistical analysis

The student t-test was used for the analysis of efficiency of ATMT transformation including temperature and duration of incubation. A *p*-value of <0.05 was considered significant.

2.9. Nucleotide sequence accession numbers

The nucleotide sequence of *PdURE1* and *PpURE1* were deposited in GenBank under accession numbers KP195072 and KP195073, respectively.

3. Results

3.1. Identification of the Pd/Pp URE1 gene and bioinformatic analyses

Based on *Pd/Pp* genome databases and sequence alignments, putative urease orthologues, designated *PdURE1* and *PpURE1* were obtained. The coding sequences of *PdURE1* spans 3127 bp, corresponding to a predicted open reading frame of 837 amino acids, consisting of six exons interrupted by five introns (KP195072). In contrast, the sequence of *PpURE1* spans 3904 bp coding for a predicted open reading frame of 882 amino acids with six exons and five introns (KP195073). The putative amino acid sequence of *PdURE1* shared 94% identity with putative *PpURE1*, and close homology to the metallo-dependent urease of *Glarea lozoyensis* ATCC 20868 (EPE30823, 77% identity). A similar level of identity was also noted with the putative urease of *Trichoderma reesei* QM6a (GenBank accession no. EGR47585, 75% identity) and *C. posadasii* 735 (GenBank accession no. AAC49868, 71% identity). The sequences also showed conservation of all of the histidine residues thought to be involved in binding to the nickel metallocenter, binding to the substrate, and catalysis (Cox et al., 2000) (Fig. 1A). These results strengthened the observation that *URE1* gene function in urea metabolism is conserved across fungal species,

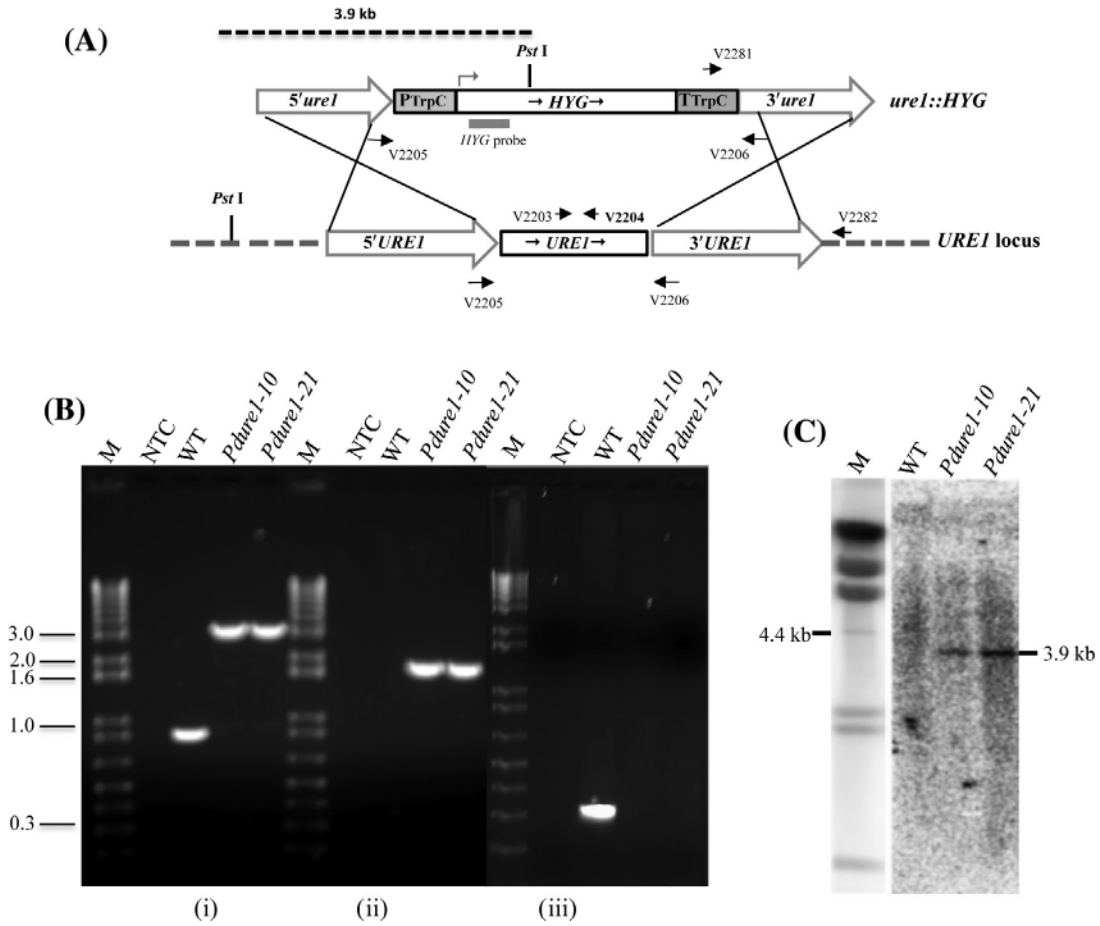

Fig. 3. Disruption of *Pd URE1* by ATMT. (A) Restriction map of the *Pdure1*-disruption cassette. 5′*URE1* (1.4 kb) and 3′*URE1* (1.5 kb) were cloned into pRF-HU2 flanking hygromycin B resistance (*HYG*) gene under the control of *Aspergillus nidulans* promoter (PTrpC) and terminator (TTrpC). The arrows represent primers used for PCR and solid gray line represent *HYG* probe used for Southern analysis. The dashed line (thick) represents genomic sequences outside of the disruption cassette. The location of restriction enzyme *Pst*I within the *HYG* gene of the disruption cassette and at the 5′ end of the *URE1* locus, outside of the disruption cassette is shown. The dashed line (thin) represents expected size product for mutant strains following enzyme digestion and Southern analysis. (B) Analysis of *ure1* transformants by PCR. Primer pair (V2205–V2206) targeting *URE1* flanking *HYG* gene (Bi-3.0 kb in size for mutants and 860 bp in size for WT), primer pair (V2281–V2282) located in the *HYG* gene and right border of the *URE1* gene (Bii-1.8 kb in size for mutants and no PCR amplicon for WT), and primer pair (V2203-V2204) located within the deletion region of *URE1* gene (Biii-318 bp in size for WT and no PCR amplicon for mutants). (C) Southern hybridization analysis. Genomic DNA from the WT and the mutant strains was digested with *Pst*I and hybridized with *HYG* probe (3.9 kb band for both the mutants and no band for the WT).

including cold-adapted fungi. The phylogenetic analysis using neighbor-joining method (Saitou and Nei, 1987) revealed that *PdURE1* clustered closely together with the ortholog of *PpURE1*, consistent with their common origin within the *Pseudeurotiaceae* (Fig. 1B).

3.2. Optimization of ATMT for Pd and Pp

Prior to experimental procedures with ATMT, the hygromycin B (HygB) minimum inhibitory concentration was determined for *Pd* and *Pp*. Hygromycin concentration of 100 μg/ml showed complete inhibition of the growth of both *Pd* and *Pp*, whereas a hygromycin concentration of 75 μg/ml showed restricted growth of both these fungi (data not shown). Other antibiotics tested, including cefotaxime (200 μg/ml) and kanamycin (50 μg/ml), did not have any adverse effect on the growth of either *Pd* or *Pp* (data not shown).

To determine whether acetosyringone (AS), a natural wound response molecule, is essential for the ATMT of *Pd* or *Pp*, this chemical was removed from the IM medium in which the *Agrobacterium* cells were grown prior to co-cultivation or was removed from the co-cultivation medium. *Pd* or *Pp* Hyg$^+$ transformants were not recovered in the absence of AS, suggesting that this inducer molecule is critical for ATMT of both *Pd* and *Pp*. In the presence of AS and at a ratio of 1:10 *Pd* or *Pp* conidia and AGL-1 cells carrying either *Pdure1::HYG* or *Ppure1::HYG* plasmid, a minimum of 24 h to 36 h of co-cultivation was required to obtain *Pd* and *Pp* Hyg$^+$ transformants (1–4 per 3 nitrocellulose membranes), respectively. However, the yields of Hyg$^+$ transformants were substantially increased when the co-cultivation period was extended to 72 h for *Pp* ($p < 0.01$) and 96 h for *Pd* ($p < 0.01$) (Fig. 2A and B).

Next, we determined the influence of co-cultivation temperature on ATMT efficiency. The 1:10 ratio of fungal conidia and AGL-1 cells spread on membranes were incubated at various temperatures for 72 h, followed by transfer of these membranes to selection medium (Fig. 2C and D). The optimal temperature for the recovery of *Pd* Hyg$^+$ transformants ranged from 15 to 18 °C. Temperatures below 15 °C or above 18 °C were detrimental to the recovery of *Pd* transformants (Fig. 2C). In contrast, the optimal temperature for recovery of *Pp* Hyg$^+$ transformants was 25 °C, followed by 20 °C. The recovery of *Pp* transformants at 15 °C was comparable to that of *Pd* transformants, but temperatures below 15 °C or above 25 °C were detrimental to the recovery of *Pp* transformants (Fig. 2D).

Finally, based on ATMT optimizations, the co-cultivation duration of 72 h was used for both *Pd* and *Pp* and co-cultivation temperatures of 15 °C for *Pd* and 25 °C for *Pp* were used. A total of 620 *Pd* Hyg$^+$ transformants and 1800 *Pp* Hyg$^+$ transformants were obtained from cultivation of approximately 1×10^7 cells in each conidial suspension, providing transformant yield of 0.006% and 0.018% for *Pd* and *Pp*, respectively.

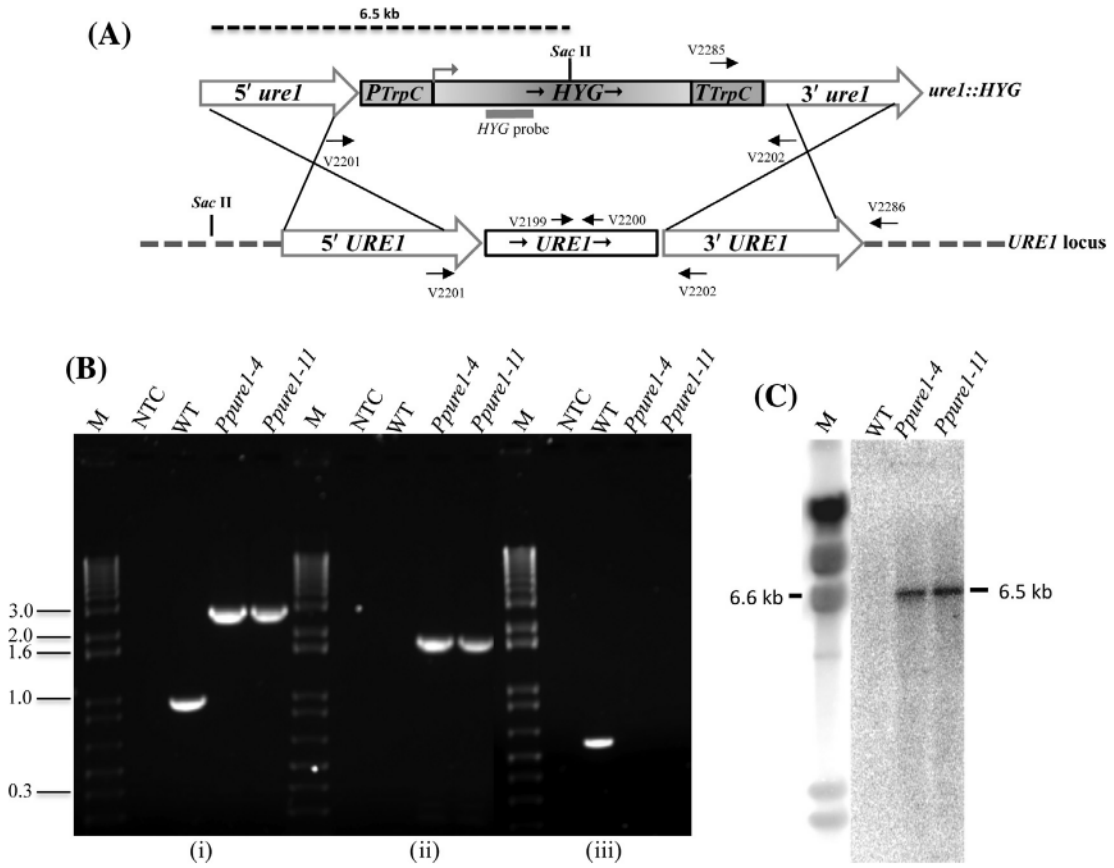

Fig. 4. Disruption of *PpURE1* by ATMT. (A) Restriction map of the *Ppure1*-disruption cassette. 5′*Ure1* (1.5 kb) and 3′*Ure1* (1.5 kb) were cloned into pRF-HU2 flanking hygromycin B resistance (*HYG*) gene under the control of *Aspergillus nidulans* promoter (PTrpC) and terminator (TTrpC). The arrows represent primers used for PCR and solid gray line represents *HYG* probe used for Southern analysis. The dashed line represents genomic sequences outside of the disruption cassette. The location of restriction enzyme *Sac*II within the *HYG* gene and at the 5′ end of the *URE1* locus, outside of the disruption cassette is shown. (B) Analysis of *ure1* transformants by PCR. Primer pair (V2201–V2202) targeting *URE1* flanking *HYG* gene (Bi-957 bp in size for WT and 2694 bp in size for mutant strains), primer pairs (V2285–V2286) located in the *HYG* gene and in the right border of *URE1* gene (Bii-1.6 kb in size for mutants and no PCR amplicon for WT), and primer pair (V2199–V220) within the deletion region of *URE1* gene (Biii-466 bp in size for WT and no PCR amplicon for mutants). (C) Southern hybridization analysis. Genomic DNA from the WT and the mutant strains was digested with *Sac*II and hybridized with *HYG* probe (6.4 kb band for both the mutants and no band for the WT).

3.3. Disruption of PdURE1 and PpURE1 genes

Of 128 putative Hyg$^+$ *Pd* transformants analyzed by PCR with primer set (V2205–V2206) targeting *URE1* flanking *HYG* gene, four displayed a single amplicon of 3000 bp in size, whereas the WT strain displayed a single amplicon of 800 bp in size, indicative of a homologous transformation of 3.1%. Results of the single integration event are shown for two of these mutants (Fig. 3A and Bi). All other transformants had two amplicons of 860 bp and 3000 bp in size, indicative of ectopic integration (data not shown). The transformants that had single amplicon were further confirmed for the integration of *Pdure1::HYG* at the homologous site by two additional primer sets. The primer set (V2281–V2282) located within the *HYG* gene and on the right border outside of the disruption cassette, yielded a 1.8 kb PCR amplicon for mutants, but not for the WT strain (Fig. 3A and Bii). The primer set (V2203-V2204) located within the deleted region of *URE1* yielded a 318-bp PCR amplicon for WT strain, but not for mutants (Fig. 3A and Biii). These mutants were passed through several generations of growth on YPD agar, which is a rich non-selective medium and thus, likely to facilitate the loss of any unstable genetic constructs. Southern hybridization of *Pst*I digested gDNA yielded single band of 3.9 kb for both the mutants, further confirming gene replacement at the homologous site without ectopic integration (Fig. 3A and C). These mutants were labeled as *Pdure1–10* and *Pdure1–21*. The rationale for selection of two *Pdure1* mutants was to test if both mutants had consistent phenotypes, as these mutants did not contain a functional *URE1*.

Of 36 *Pp* Hyg$^+$ transformants analyzed by PCR with primer set (V2201–V2202) targeting *URE1* flanking *HYG* gene, six displayed a single amplicon of 2694 bp in size, whereas the WT strain had a single amplicon of 957 bp in size, indicative of a homologous integration of 16.7%. Results of the single integration event are shown for two of these mutants (Fig. 4A and Bi). All other Hyg$^+$ *Pp* transformants had two amplicons of 957 bp and 2694 bp in size, indicative of ectopic integration (data not shown). Two of the six mutants were further confirmed for *URE1* deletion at the homologous site by additional primer sets as described for *Pd* (Fig. 4A and Bii–iii). The Southern analysis of gDNA digested with *Sac*II revealed a single band of expected size of 6.5. kb in both the mutant strains, further confirming gene replacement at the homologous site without ectopic integration (Fig. 4A and C). These mutants were labeled as *Ppure1–4* and *Ppure1–11*, and the rationale for selection of two *Ppure1* mutants was same as described above for *Pdure1*.

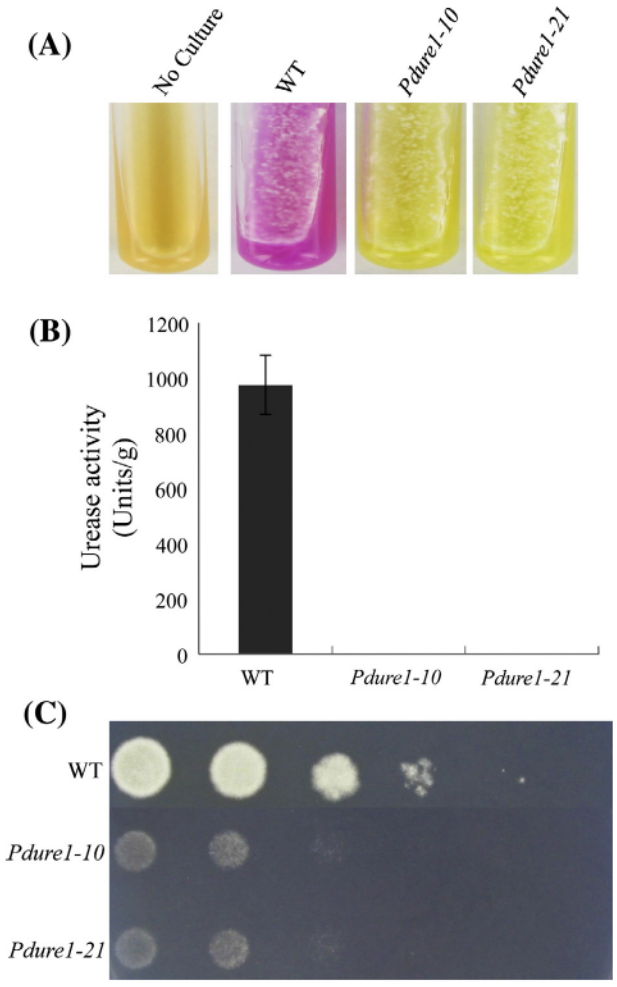

Fig. 5. Characterization of *Pdure1* mutants. (A) Approximately 10 µl aliquot of *Pd* conidial suspensions (10^7/ml) from WT and mutant strains were placed on Christensen's urea agar and incubated for 2 weeks at 15 °C. Absence of the magenta color with mutant strains indicated loss of urease enzyme activity. Tube without culture served as quality control for medium. (B) The urease enzyme activity from cell lysates was determined according to the Urease Assay Kit (BioAssay Systems). The mutant strains did not produce urease enzyme while WT did. C) Approximately 10 µl aliquot of the dilution series of conidial suspensions of the WT and *Pdure1* mutant strains were spotted on two separate YNB-U agar plates to avoid any residual effect of the growth of WT strain on the mutant strains. Plates were incubated at 15 °C for 7-days. A significant difference of growth between mutant and WT strains confirmed that *URE1* is required when nitrogen is the sole source of nutrient.

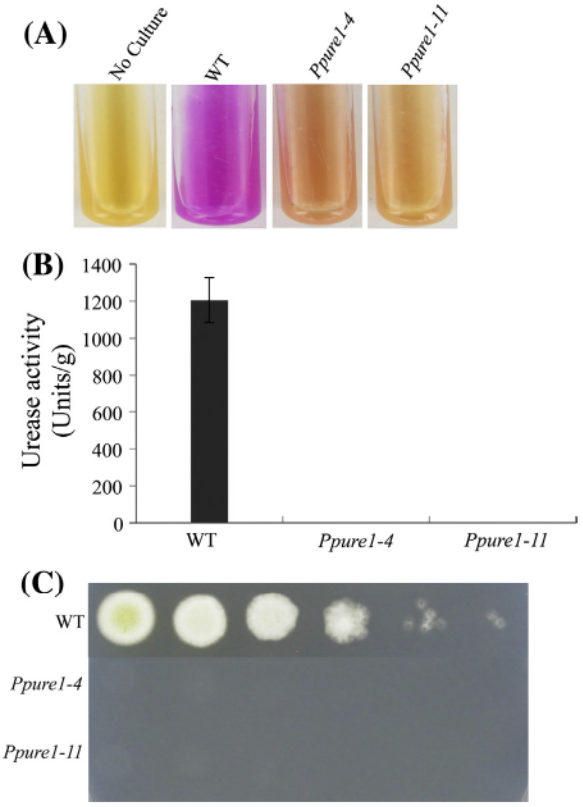

Fig. 6. Characterization of *Ppure1* mutants. (A) Approximately 10 µl aliquots of *Pp* conidial suspensions from the WT and mutant strains were placed on Christensen's urea agar and incubated for 2 weeks at 15 °C. Absence of the magenta color with mutant strains indicated loss of urease enzyme activity. Tube without culture served as quality control for medium. (B) The urease enzyme activity from cell lysates was determined according to Urease Assay Kit (BioAssay Systems). The *Ppure1* mutants did not produce urease enzyme while WT did. (C) Approximately 10 µl aliquots of dilution series of the conidial suspensions of the WT and mutant strains were spotted on two separate YNB-U agar plates to avoid any residual effect of the growth of WT strain on the mutant strains. Plates were incubated at 15 °C for a 7-day period. No growth of mutants indicated that the *URE1* is required when nitrogen is the sole source of nutrient.

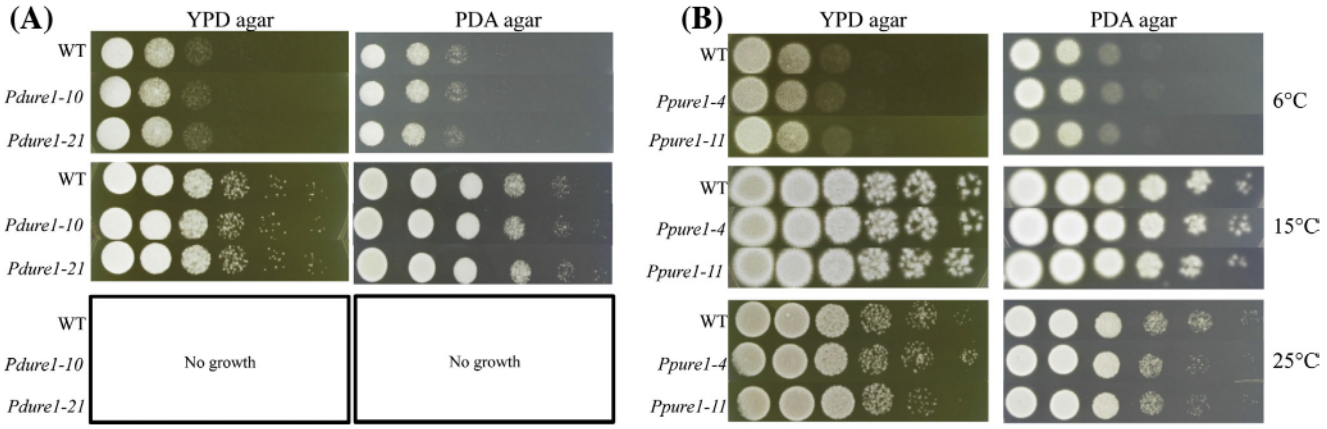

Fig. 7. Growth of *Pdure1* and *Ppure1* mutants at different temperatures. (A) Approximately 10 μl aliquots of the dilution series of the conidial suspension of WT and *Pdure1* mutant strains were spotted on YPD and PDA agar. Plates were incubated at 6 °C for 14-day, and at 15 °C and 25 °C for 7-day periods. No growth of the WT and mutant strains observed at 25 °C. (B) Approximately 10 μl aliquots of the dilution series of the conidial suspension of *Pp* WT and *Ppure1* mutant strains were spotted on YPD and PDA agar. Plates were incubated at 6 °C for 14-day, and at 15 °C and 25 °C for 7-day periods. Excellent growth of both *Pp* WT and *Ppure1* mutant strains was observed at all temperatures tested.

The *Pdure1* and *Ppure1* mutants were assessed for urease enzyme activity along with their respective WT strains. It was interesting to note that the *Pd* WT and *Pdure1* mutant strains grew relatively better than the *Pp* WT and *Ppure1* mutant strains on Christensen's urea agar. Despite growth differences, no color development after 2 weeks of incubation, confirmed that the *URE1* gene was functionally deleted in both *Pdure1* and *Ppure1* mutants (Figs. 5A and 6A). These results were further corroborated by measurements of urease enzyme activity in cell lysates prepared from *Pdure1* or *Ppure1* mutants. Urease activity of the WT strains of *Pd* and *Pp* was 974 ± 113 U/g and 1205 ± 121 U/g, respectively. In contrast, urease activity was undetectable in *Pdure1* and *Ppure1* mutants (Figs. 5B and 6B). Finally, we tested whether the *URE1* gene is involved in urea metabolism in these two organisms. *Ppure1* mutants failed to grow on YNB-U as compared to the *Pp* WT strain (Fig. 6C). In contrast, poor but detectable growth of *Pdure1* mutants was observed on YNB-U (Fig. 5C). To further analyze this discrepant result, we tested *Pd* WT and *Pdure1* mutant strains on YNB agar devoid of urea. Similar poor growth of WT and mutant strains observed indicating that the glucose in the YNB medium possibly supports minimal growth of *Pd* but not *Pp* strains (Supplementary Fig. S2). These results further corroborated our findings regarding *Pdure1* mutants, as *Ppure1* mutants were unable to utilize urea, confirming that the *URE1* gene is involved in urea metabolism in both *Pd* and *Pp*.

3.4. Growth and sporulation

The *URE1* gene was found to be dispensable for the growth of *Pd* or *Pp*, as *Pdure1* mutants grew efficiently on YPD and PDA media between 6 and 15 °C while *Ppure1* mutants grew as well between 6 and 25 °C (Fig. 7). Similarly, *URE1* gene was not required for sporulation, as both *Pdure1* and *Ppure1* mutants produced spores as efficiently as their respective WT strains on PDA agar (Supplementary Fig. S3). These results indicated that *URE1* is dispensable for both cold adaptation and sporulation in *Pd* and *Pp*.

4. Discussion

The highlight of this study was the successful use of the ATMT system for targeted gene disruption in cold-adapted fungi *P. destructans* (*Pd*) and *P. pannorum* (*Pp*). Among the parameters studied for ATMT, the incubation temperature seems to be the critical factor in the transformation of *Pd* and *Pp*. These results are not surprising as *Pd* is a psychrophilic fungus, which grows best between 15 °C and 18 °C (Chaturvedi et al., 2010; Verant et al., 2012). The temperature below 20 °C has been shown to be detrimental to the expression of some *vir* (tumor forming) genes of *Agrobacterium* necessary for pilus production and conjugation for T-DNA transfer from donor to recipient cells (Fullner and Nester, 1996; Baron et al., 2001; Sugui et al., 2005 #871). Apart from temperature, *Agrobacterium*-mediated transformation showed strong correlation with the duration of co-cultivation and the presence of AS. These results are in agreement with other fungal pathogens indicating that the pathways leading to T-DNA insertion are conserved across fungal species (Piers et al., 1996; Gouka et al., 1999; Abuodeh et al., 2000; Yamada et al., 2009).

We also found that homologous gene integration was lower in *Pd* (3.1%) than in *Pp* (16.7%). It is important to point out that the homologous arm of the *URE1* gene was chosen from the same strain used for transformation, as strict sequence identity is required for high efficiency homologous recombination in other fungal pathogens (Sudarshan et al., 1999; Narasipura et al., 2003, 2005). The G+C content appears to be identical between *Pd* and *Pp* (Chibucos et al., 2013), such that this does not appear to be a likely factor affecting low homologous gene integration observed in *Pd*.

The availability of a simple phenotypic test (color change in Christensen's urea agar) was a consideration for choosing the *URE1* gene encoding urease for gene disruption studies in the present investigation. Others and we have demonstrated that *Pd* secretes a large amount of urease into the growth medium (Chaturvedi et al., 2010; Raudabaugh and Miller, 2013). The role of urease in the fungal and bacterial virulence has been investigated using different vertebrate models (Jones et al., 1990; Eaton et al., 1991; Cox et al., 2000; Mirbod-Donovan et al., 2006). Currently, there are no laboratory models available for WNS or for testing the pathogenic potential of *Pdure1* and *Ppure1* mutant strains. Although, a recent study demonstrated that experimentally infected bats with *Pd* develop WNS (Lorch et al., 2011), the set-up described is not amenable to fungal mutant comparisons in the laboratory. Therefore, the evaluation of the role of urease in the virulence of *Pd* and *Pp* awaits the availability of *in vivo* or *ex vivo* model.

Acknowledgments

This study was partly supported with funds from the National Science Foundation (16-0039-01). We are grateful to Dr.

Seogchan Kang (University Park, PA, USA) for providing *Agrobacterium tumefaciens* AGL-1 strain. Dr. Rasmus JN Frandsen (Frederiksberg, Denmark) is thanked for the generous gift of plasmid pRF-HU2. We also thank Dr. Harry Taber for the editing of the manuscript.

Appendix A. Supplementary material

Supplementary data associated with this article can be found, in the online version, at http://dx.doi.org/10.1016/j.fgb.2015.05.009.

References

Abuodeh, R.O., Orbach, M.J., Mandel, M.A., Das, A., Galgiani, J.N., 2000. Genetic transformation of *Coccidioides immitis* facilitated by *Agrobacterium tumefaciens*. J. Infect. Dis. 181, 2106–2110.

Baron, C., Domke, N., Beinhofer, M., Hapfelmeier, S., 2001. Elevated temperature differentially affects virulence, VirB protein accumulation, and T-pilus formation in different *Agrobacterium tumefaciens* and *Agrobacterium vitis* strains. J. Bacteriol. 183, 6852–6861.

Blehert, D.S., 2012. Fungal disease and the developing story of bat white-nose syndrome. PLoS Pathogens 8, e1002779.

Blehert, D.S., Hicks, A.C., Behr, M., et al., 2009. Bat white-nose syndrome: an emerging fungal pathogen? Science 323, 227.

Chaturvedi, V., Springer, D.J., Behr, M.J., et al., 2010. Morphological and molecular characterizations of psychrophilic fungus *Geomyces destructans* from New York bats with White Nose Syndrome (WNS). PLoS One 5, e10783.

Chibucos, M.C., Crabtree, J., Nagaraj, S., Chaturvedi, S., Chaturvedi, V., 2013. Draft Genome Sequences of Human Pathogenic Fungus *Geomyces pannorum Sensu Lato* and Bat White Nose Syndrome Pathogen *Geomyces* (*Pseudogymnoascus*) *destructans*. Genome Announcement 1, e01045–01013.

Cox, G.M., Mukherjee, J., Cole, G.T., Casadevall, A., Perfect, J.R., 2000. Urease as a virulence factor in experimental cryptococcosis. Infect. Immun. 68, 443–448.

Dobinson, K.F., Grant, S.J., Kang, S., 2004. Cloning and targeted disruption via *Agrobacterium tumefaciens*-mediated transformation of a trypsin protease gene from the vascular wilt fungus *Verticillium dohliae*. Curr. Genet. 45, 104–110.

Dogan, R.I., Getoor, L., Wilbur, W.J., Mount, S.M., 2007. SplicePort – an interactive splice-site analysis tool. Nucleic Acids Res. 35, W285–291.

Eaton, K.A., Brooks, C.L., Morgan, D.R., Krakowka, S., 1991. Essential role of urease in pathogenesis of gastritis induced by *Helicobacter pylori* in gnotobiotic piglets. Infect. Immun. 59, 2470–2475.

Eckert, M., Maguire, K., Urban, M., Foster, S., Fitt, B., Lucas, J., Hammond-Kosack, K., 2005. *Agrobacterium tumefaciens*-mediated transformation of *Leptosphaeria* spp. and *Oculimacula* spp. with the reef coral gene DsRed and the jellyfish gene gfp. FEMS Microbiol. Lett. 253, 67–74.

Frandsen, R.J.N., 2011. A guide to binary vectors and strategies for targeted genome modification in fungi using *Agrobacterium tumefaciens*-mediated transformation. J. Microbiol. Methods 87, 247–262.

Frandsen, R.J., Andersson, J.A., Kristensen, M.B., Giese, H., 2008. Efficient four fragment cloning for the construction of vectors for targeted gene replacement in filamentous fungi. BMC Mol. Biol. 9, 70.

Frick, W.F., Pollock, J.F., Hicks, A.C., Langwig, K.E., Reynolds, D.S., Turner, G.G., Butchkoski, C.M., Kunz, T.H., 2010. An emerging disease causes regional population collapse of a common North American bat species. Science 329, 679–682.

Fullner, K.J., Nester, E.W., 1996. Temperature affects the T-DNA transfer machinery of *Agrobacterium tumefaciens*. J. Bacteriol. 178, 1498–1504.

Gouka, R.J., Gerk, C., Hooykaas, P.J., Bundock, P., Musters, W., Verrips, C.T., de Groot, M.J., 1999. Transformation of *Aspergillus awamori* by *Agrobacterium tumefaciens*-mediated homologous recombination. Nat. Biotechnol. 17, 598–601.

Helber, N., Requena, N., 2008. Expression of the fluorescence markers DsRed and GFP fused to a nuclear localization signal in the arbuscular mycorrhizal fungus *Glomus intraradices*. New Phytol. 177, 537–548.

Jones, B.D., Lockatell, C.V., Johnson, D.E., Warren, J.W., Mobley, H.L., 1990. Construction of a urease-negative mutant of *Proteus mirabilis*: analysis of virulence in a mouse model of ascending urinary tract infection. Infect. Immun. 58, 1120–1123.

Katoh, K., Asimenos, G., Toh, H., 2009. Multiple alignment of DNA sequences with MAFFT. Methods Mol. Biol. 537, 39–64.

Lorch, J.M., Meteyer, C.U., Behr, M.J., et al., 2011. Experimental infection of bats with *Geomyces destructans* causes white-nose syndrome. Nature 480, 376–378.

McClelland, C.M., Chang, Y.C., Kwon-Chung, K.J., 2005. High frequency transformation of *Cryptococcus neoformans* and *Cryptococcus gattii* by *Agrobacterium tumefaciens*. Fungal Genet. Biol. 42, 904–913.

Michielse, C.B., Hooykaas, P.J., van den Hondel, C.A., Ram, A.F., 2005. *Agrobacterium*-mediated transformation as a tool for functional genomics in fungi. Curr. Genet. 48, 1–17.

Minnis, A.M., Lindner, D.L., 2013. Phylogenetic evaluation of *Geomyces* and allies reveals no close relatives of *Pseudogymnoascus destructans*, comb. nov., in bat hibernacula of eastern North America. Fungal Biol. 117, 638–649.

Mirbod-Donovan, F., Schaller, R., Hung, C.Y., Xue, J., Reichard, U., Cole, G.T., 2006. Urease produced by *Coccidioides posadasii* contributes to the virulence of this respiratory pathogen. Infect. Immun. 74, 504–515.

Möller, E.M., Bahnweg, G., Sandermann, H., Geiger, H.H., 1992. A simple and efficient protocol for isolation of high molecular weight DNA from filamentous fungi, fruit bodies, and infected plant tissues. Nucleic Acids Res. 20, 6115–6116.

Mozo, T., Hooykaas, P.J., 1991. Electroporation of mega plasmids into *Agrobacterium*. Plant Mol. Biol. 16, 917–918.

Mullins, E.D., Chen, X., Romaine, C.P., Raina, R., Geiser, D.M., Kang, S., 2001. *Agrobacterium*-mediated transformation of *Fusarium oxysporum*: an efficient tool for insertional mutagenesis and gene transfer. Phytopathology 91, 173–180.

Narasipura, S.D., Ault, J.G., Behr, M.J., Chaturvedi, V., Chaturvedi, S., 2003. Characterization of Cu, Zn superoxide dismutase (SOD1) gene knockout mutant of *Cryptococcus neoformans* var. *gattii*: role in biology and virulence. Mol. Microbiol. 47, 1681–1694.

Narasipura, S.D., Chaturvedi, V., Chaturvedi, S., 2005. Characterization of *Cryptococcus neoformans* var. *gattii SOD2* reveals distinct roles of the two superoxide dismutases in fungal biology and virulence. Mol. Microbiol. 55, 1782–1800.

Olszewski, M.A., Noverr, M.C., Chen, G.H., Toews, G.E., Cox, G.M., Perfect, J., Huffnagle, G.B., 2004. Urease expression by *Cryptococcus neoformans* promotes microvascular sequestration, thereby enhancing central nervous system invasion. Am. J. Pathol. 164, 1761–1771.

Piers, K.L., Heath, J.D., Liang, X., Stephens, K.M., Nester, E.W., 1996. *Agrobacterium tumefaciens*-mediated transformation of yeast. Proc. Natl. Acad. Sci. USA 93, 1613–1618.

Rajkumar, S.S., Rudd, R.J., Okoniewski, J.C., Xu, J., Chaturvedi, S., Chaturvedi, V., 2011. Dispersal of a single, clonal genotype of *Geomyces destructans* among New York bats with geomycosis (White Nose Syndrome). Emerg. Infect. Dis. 17, 1273–1276.

Raudabaugh, D.B., Miller, A.N., 2013. Nutritional capability of and substrate suitability for *Pseudogymnoascus destructans*, the causal agent of bat White-Nose Syndrome. PLoS One 8, e78300.

Ren, P., Haman, K.H., Last, L.A., Rajkumar, S.S., Keel, M.K., Chaturvedi, V., 2012. Clonal spread of *Geomyces destructans* among bats, Midwestern and Southern United States. Emerg. Infect. Dis. 18, 883–885.

Reynolds, H.T., Barton, H.A., 2014. Comparison of the white-nose syndrome agent *Pseudogymnoascus destructans* to cave-dwelling relatives suggests reduced saprotrophic enzyme activity. PLoS One 9, e86437.

Saitou, N., Nei, M., 1987. The neighbor-joining method: a new method for reconstructing phylogenetic trees. Mol. Biol. Evol. 4, 406–425.

Stanke, M., Morgenstern, B., 2005. AUGUSTUS: a web server for gene prediction in eukaryotes that allows user-defined constraints. Nucleic Acids Res. 33, W465–467.

Stanke, M., Steinkamp, R., Waack, S., Morgenstern, B., 2004. AUGUSTUS: a web server for gene finding in eukaryotes. Nucleic Acids Res. 32, W309–312.

Sugui, J.A., Chang, Y.C., Kwon-Chung, K.J., 2005. *Agrobacterium tumefaciens*-mediated transformation of *Aspergillus fumigatus*: an efficient tool for insertional mutagenesis and targeted gene disruption. Appl. Environ. Microbiol. 71, 1798–1802.

Sudarshan, S., Davidson, R.C., Heitman, J., Alspaugh, J.A., 1999. Molecular analysis of the *Cryptococcus neoformans ADE2* gene, a selectable marker for transformation and gene disruption. Fungal Genet. Biol. 27, 36–48.

Tamura, K., Dudley, J., Nei, M., Kumar, S., 2007. MEGA4: Molecular Evolutionary Genetics Analysis (MEGA) software version 4.0. Mol. Biol. Evol. 24, 1596–1599.

Tsuda, M., Karita, M., Morshed, M.G., Okita, K., Nakazawa, T., 1994. A urease-negative mutant of *Helicobacter pylori* constructed by allelic exchange mutagenesis lacks the ability to colonize the nude mouse stomach. Infect. Immun. 62, 3586–3589.

Verant, M.L., Boyles, J.G., Waldrep, W.J., Wibbelt, G., Blehert, D.S., 2012. Temperature-dependent growth of *Geomyces destructans*, the fungus that causes bat white-nose syndrome. PLoS One 7, e46280.

Yamada, T., Makimura, K., Satoh, K., Umeda, Y., Ishihara, Y., Abe, S., 2009. *Agrobacterium tumefaciens*-mediated transformation of the dermatophyte, *Trichophyton mentagrophytes*: an efficient tool for gene transfer. Med. Mycol. 47, 485–494.

Zhang, T., Zhuo, Y., Jia, X., Liu, J., Gao, H., Song, F., Liu, M., Zhang, L., 2013. Cloning and characterization of the gene cluster required for beauvericin biosynthesis in *Fusarium proliferatum*. Sci. China Life Sci. 56, 628–637.